5696 J. Med. Chem. 2010, 53, 5696–5706
DOI: 10.1021/jm100479q

Journal of Medicinal Chemistry Article

Synthesis and in Vivo Evaluation of Phenethylpiperazine Amides: Selective 5-Hydroxytryptamine$_{2A}$ Receptor Antagonists for the Treatment of Insomnia

Yifeng Xiong,* Brett Ullman, Jin-Sun Karoline Choi, Martin Cherrier, Sonja Strah-Pleynet, Marc Decaire, Peter I. Dosa, Konrad Feichtinger, Bradley R. Teegarden, John M. Frazer, Woo H. Yoon, Yun Shan, Kevin Whelan, Erin K. Hauser, Andrew J. Grottick, Graeme Semple, and Hussien Al-Shamma

Arena Pharmaceuticals, 6166 Nancy Ridge Drive, San Diego, California 92121

Received April 19, 2010

Recent developments in sleep research suggest that antagonism of the serotonin 5-HT$_{2A}$ receptor may improve sleep maintenance insomnia. We herein report the discovery of a series of potent and selective serotonin 5-HT$_{2A}$ receptor antagonists based on a phenethylpiperazine amide core structure. When tested in a rat sleep pharmacology model, these compounds increased both sleep consolidation and deep sleep. Within this series of compounds, an improvement in the metabolic stability of early leads was achieved by introducing a carbonyl group into the phenethylpiperazine linker. Of note, compounds **14** and **27** exhibited potent 5-HT$_{2A}$ receptor binding affinity, high selectivity over the 5-HT$_{2C}$ receptor, favorable CNS partitioning, and good pharmacokinetic and early safety profiles. In vivo, these two compounds showed dose-dependent, statistically significant improvements on deep sleep (δ power) and sleep consolidation at doses as low as 0.1 mg/kg.

Introduction

The involvement of serotonin (5-HT[a]) in the regulation of sleep and wakefulness has been well documented.[1] 5-HT actions in the central nervous system (CNS) are mediated by multiple receptor subtypes that are classified into seven subfamilies.[2] Of particular interest here is the 5-HT$_2$ subfamily, which includes three subtypes: 5-HT$_{2A}$, 5-HT$_{2B}$, and 5-HT$_{2C}$. Among these three receptors, only 5-HT$_{2A}$ and 5-HT$_{2C}$ are distributed in areas of the CNS that are implicated in the regulation of sleep and waking.[3] Furthermore, recent preclinical and clinical evidence suggests that 5-HT$_{2A}$ antagonism might be effective in the treatment of sleep maintenance insomnia.[4] Indeed, several selective 5-HT$_{2A}$ antagonists have entered clinical development for the treatment of insomnia including eplivanserin, volinanserin, pruvanserin, and nelotanserin.[5]

We recently reported the discovery, synthesis, and associated structure−activity relationship (SAR) of nelotanserin (APD125) (Figure 1), a phenylpyrazole urea based selective 5-HT$_{2A}$ inverse agonist that was advanced into clinical trials for the treatment of insomnia.[6] In preclinical studies, nelotanserin induced dose-dependent sleep consolidation effects and increased markers of deep slow wave sleep (SWS) in rats.[7] In clinical studies, nelotanserin was well tolerated and improved multiple objective parameters of sleep maintenance and sleep consolidation in adults with primary chronic insomnia.[8]

Following our discovery of nelotanserin, medicinal chemistry efforts were focused on identifying backup compounds suitable for development. Nelotanserin and related molecules still retained high 5-HT$_{2A}$ receptor affinity despite lacking a basic nitrogen group. Unfortunately, such molecules have little or no aqueous solubility. To address this, a backup program was initiated with the goal of improving aqueous solubility, and consequently pharmaceutical properties, while maintaining receptor activity and selectivity and with a benign safety profile similar to that of nelotanserin. Phenethylpiperazine is a common motif to many 5-HT$_{2A}$ receptor antagonists (Figure 1);[9,10] it contains a readily protonatable amine that can greatly increase aqueous solubility. For these reasons we decided to introduce this motif into our internally discovered phenylpyrazole scaffold. This scaffold has also yielded another potent 5-HT$_{2A}$ receptor inverse agonist, APD791, which was advanced into clinical trials as a potential treatment for arterial thrombosis.[11,12] Keeping the phenylpyrazole portion of nelotanserin but replacing the 2,4-difluorophenyl urea with a 4-fluorophenethylpiperazine urea gave **2** (Figure 2). Compound **2** maintained modest receptor affinity but had 300-fold lower affinity than nelotanserin (Table 1). It was reasoned that the distance between the two lipophilic portions, the distal phenyl ring and the phenylpyrazole moiety, may be too great. To this end the phenyl group from the phenylpyrazole moiety was removed to provide **3**. Urea **3** showed a slight increase in the 5-HT$_{2A}$ receptor affinity but was still 170-fold weaker than nelotanserin. Compound **3** was then further modified from a urea to an amide to give **4**. Strikingly, amide **4** had 20-fold higher affinity than **3** (K_i = 3.6 nM, Table 1) and was now of comparable affinity to nelotanserin. In addition it had excellent selectivity for the 5-HT$_{2A}$ receptor over the 5-HT$_{2C}$

*To whom correspondence should be addressed. Phone: +1 858-453-7200. Fax: +1 858-453-7210. E-mail: yxiong@arenapharm.com.

[a] Abbrevations: 5-HT, serotonin; CNS, central nervous system; iv; intravenous; SAR, structure−activity relationship; DOI, 2,5-dimethoxy-4-iodoamphetamine; hERG, human ether-a-go-go-related gene; REM, rapid eye movement; NREM, nonrapid eye movement; HATU, *N*,*N*,*N*′,*N*′-tetramethyl-*O*-(7-azabenzotriazol-1-yl)uronium hexafluorophosphate; EEG, electroencephalograph; EMG, electromyography; mp, melting point; rt, room temperature; DSC, differential scanning calorimetry; PXRD, powder X-ray diffraction.

 Published on Web 07/12/2010

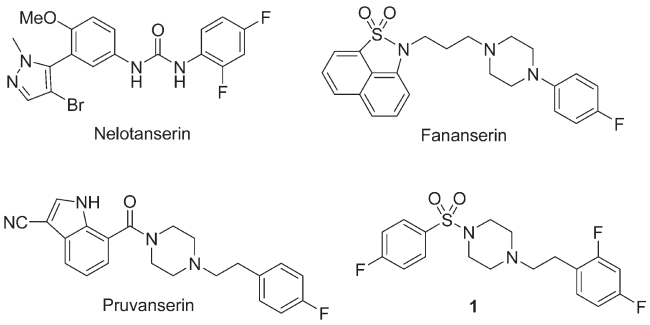

Figure 1. Nelotanserin and selected piperazine-containing 5-HT_{2A} receptor antagonists.

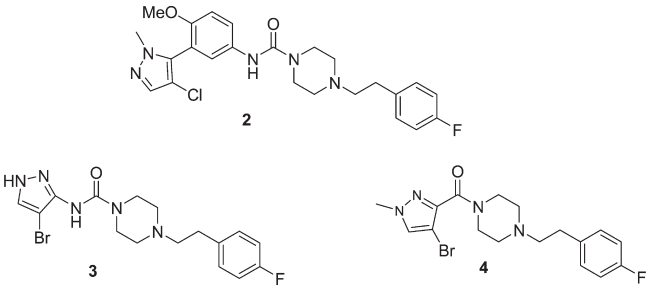

Figure 2. Evolution of phenethylpiperazine-based 5-HT_{2A} receptor antagonists.

receptor, better in fact than that for nelotanserin. More importantly, it was anticipated that the aqueous solubility of compounds of structure similar to **4** should be greatly improved over nelotanserin. The approach we had taken had thus led us to new compounds by making use of the novel pyrazole moiety present in our earlier lead series, and we set about further exploration of this new series of analogues.

Pharmacokinetic assessment of **4** after a 2 mg/kg intravenous (iv) dose in rat suggested that this compound had high plasma clearance (9.3 (L/h)/kg, 220% of total hepatic blood flow) and consequently low systemic exposure (AUC 91 h·ng/mL) and oral bioavailability (9%), as shown in Table 2. In vitro metabolism studies using liver microsomes confirmed that this compound had poor stability in rat microsomes ($T_{1/2}$ = 14 min) but was relatively stable in human and other species. Evaluation of hERG channel blockade in patch clamp electrophysiology assays showed **4** gave 79% inhibition at 3 μM which raised a potential cardiovascular safety concern. To address both of these issues simultaneously, several approaches were explored, including phenyl ring substitutions, replacement of the phenyl ring with other aromatics, modification of the piperazine ethyl linker, and replacement of the pyrazole. In the following discussion, the optimization of **4** to provide **14** and **27**, two analogues with good pharmacokinetic and in vitro safety profiles, will be described.

Results and Discussion

Chemistry. Our initial chemistry strategy was to maintain the key bromopyrazole group from **4** and use this as a probe to determine the contribution to the 5-HT_{2A} receptor binding affinity provided by the phenyl ring, substituents on the phenyl ring, and ethylpiperazine linker. Starting from commercially available 4-bromopyrazole-3-carboxylic acid (Scheme 1), coupling with phenethylpiperazine or 4-fluorophenethylpiperazine (commercially available) provided **4** and **5**, respectively.

Table 1. Binding Affinities of Compounds **2**−**20** at Human 5-HT_{2A} and 5-HT_{2C} Receptors

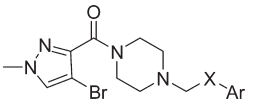

4-20

Comp.	X	Ar	5-HT_{2A} K_i[a](nM)	5-HT_{2C} K_i[a] (nM)
Pruvanserin			0.48	645
Nelotanserin			0.51	110
2			155	>10000
3			88	>10000
4	CH_2	4-F-Phenyl	3.6	4146
5	CH_2	Phenyl	68	>10000
7	CH_2	2-F-Phenyl	18	>10000
8	CH_2	3-F-Phenyl	542	>10000
9	CH_2	4-Cl-Phenyl	34	>10000
10	CH_2	4-OMe-Phenyl	408	>10000
11	CH_2	2,4-di-F-Phenyl	1.1	2820
12	CH_2	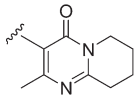	>10000	>10000
13	CH_2	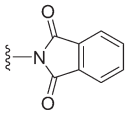	>10000	>10000
14	CO	4-F-Phenyl	3.9	2120
15	CO	2,4-di-F-Phenyl	70	>10000
16	CO	2-F-Phenyl	270	9800
17	CO	4-CF_3-Phenyl	865	>10000
18	CO	4-OCF_3-Phenyl	6000	5614
19	CHOH	4-F-Phenyl	368	>10000
20	CNOMe	4-F-Phenyl	2470	8600

[a] K_i values are the mean of at least three experiments performed in triplicate, determined from 10 concentrations. All K_i values were calculated from IC_{50} values using the method of Cheng and Prusoff[14] with standard deviation of < 0.4 log unit.

To expand the SAR on phenethylpiperazine portion, coupling of 4-bromopyrazole-3-carboxylic acid with 1-*tert*-butoxycarbonylpiperazine followed by deprotection afforded intermediate **6**. Alkylation of **6** with various substituted phenethyl bromides or chlorides provided 4-bromopyrazole derivatives **7**−**18**. The carbonyl group of phenethanone piperazines could also be reduced to the alcohol **19** or converted to the oxime **20**.[13] In vitro competitive binding assays with radiolabeled 2,5-dimethoxy-4-iodoamphetamine ([^{125}I]DOI) were used to determine K_i values for all compounds against recombinant h5-HT_{2A} and h5-HT_{2C} receptors (Table 1).

The unsubstituted phenyl derivative **5** had nearly 20-fold lower affinity in the binding assay than **4**. Switching from the *p*-fluoro to *o*-fluoro to give **7** returned some of the binding affinity, but a significant loss was observed with the fluoro group at the meta-position (**8**). This suggested that para-substitutions were most favored followed by ortho-substitutions, whereas meta-substitutions were not well tolerated. As

Table 2. Rat Pharmacokinetic Parameters of **4** and **14** after 10 mg/kg Oral Dose[a]

compd	C_{max} (ng/mL)	AUC_{last} (h·ng/mL)	$T_{1/2}$ (h)	IV CL_{total} ((L/h)/kg)	V_{ss} (L/kg)	F (%)[b]
4	48	91	1.4	9.3	8.1	9
14	1257	1450	2.1	4.0	1.5	59

[a] Values represent the mean of $n = 3$ animals. [b] F calculated relative to a 2 mg/kg iv dose.

Scheme 1. Synthesis of Compounds **4**−**20**[a]

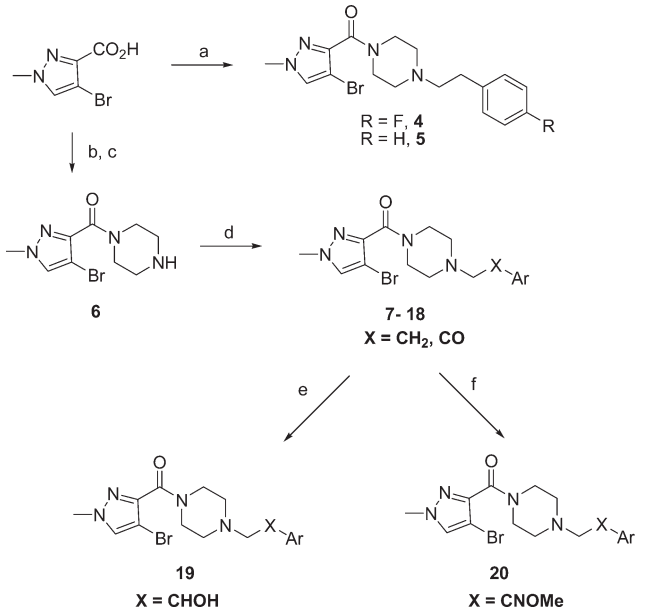

[a] Reagents and conditions: (a) 1-(4-fluorophenethyl)piperazine or phenethylpiperazine, HATU, triethylamine, THF; (b) 1-*tert*-butoxycarbonylpiperazine, triethylamine, HATU, THF; (c) HCl in dioxane, 4 N; (d) YCH_2XAr (Y = Br or Cl, X = CH_2 or CO), K_2CO_3, CH_3CN or DMF; (e) $NaBH_4$, MeOH; (f) NH_2OMe, EtOH.

a result, more para-substituents were evaluated, compounds **9** and **10** among them. Surprisingly, there was a wide range of binding affinities even within the para-substituted analogues. The closely related *p*-Cl analogue **9** had 10-fold lower affinity than **4**, and the *p*-OMe analogue **10** had a 100-fold decrease in binding affinity. Overall, the aromatic moiety of the phenethylpiperazine appeared to favor moderately lipophilic substitution. This was also confirmed by replacing the phenyl group with other aromatics that contained a polar functionality as exemplified by **12** and **13**. Both compounds had polar carboxamide groups in the aromatic moiety, and they lost all affinity for the 5-HT_{2A} receptor. One encouraging result was that 2,4-difluoro substitution of the phenyl ring, **11**, provided a modest but significant increase in 5-HT_{2A} binding affinity compared to **4**.

However, when **11** was further evaluated for stability in rat liver microsomes ($T_{1/2}$ = 9 min) and hERG activity in the patch clamp assays (80% inhibition at 3 μM), neither of these parameters were improved compared to **4**. Further microsomal stability studies were conducted on a number of phenethylpiperazine linker derivatives confirming that all of them displayed poor stability in rat. With the aromatic 4-position blocked, we reasoned that benzylic oxidation of the phenethyl group may be the root cause of this poor stability. In an attempt to block the site of benzylic oxidation, **14** was prepared where a carbonyl group was introduced at the benzylic position to give a phenethanone piperazine linker. Gratifyingly, **14** not only retained the high binding affinity at the 5-HT_{2A} receptor (Table 1) but also showed improved microsomal stability in rat ($T_{1/2}$ > 60 min). An assessment of pharmacokinetics in rat showed that all parameters had been greatly improved; **14** had good oral bioavailability (59%) and excellent exposure (AUC = 1450 h·ng/mL) following a 10 mg/kg oral dose, with a clearance rate of 4.0 (L/h)/kg (Table 2). In addition, **14** showed only 20% hERG inhibition at 3 μM in the screening assay and an IC_{50} of 19 μM when tested in the same patch clamp assay in a full concentration-response, suggesting a lower cardiovascular safety risk. Exploration of aromatic substitutions based on the phenethanone piperazine linker was carried out to determine if the *p*-fluoro or 2,4-difluoro were still the optimal substituents. Compound **15** in which the phenyl ring was substituted with a 2,4-difluoro group was prepared. In contrast to the phenethylpiperazine linker, enhanced affinity was not observed with this 2,4-difluoro substitution. Instead a 17-fold decrease in binding affinity was observed. *o*-Fluoro analogue **16** also had much weaker 5-HT_{2A} binding affinity compared to the *p*a-fluoro analogue **14**. By extrapolation from the earlier series in which para-substitution and lipophilicity were preferred at the phenyl group, attention was then drawn toward more lipophilic para-substituents. *p*-CF_3 and *p*-OCF_3 analogues (**17** and **18**) were prepared; however, both had considerably reduced 5-HT_{2A} binding affinity compared to **14**. It appeared that the binding pocket in the phenyl region may be somewhat less accommodating with the phenethanone piperazine linker than when the phenethylpiperazine linker was in place.

We tried to further explore the limits of the phenethyl linker region, where the carbonyl group was well tolerated, by preparing alcohol **19** via simple reduction of the carbonyl group of **14** and by preparing **20** by conversion of the carbonyl group to an oxime. However, as shown in Table 1, either of these modifications gave a significant reduction in the receptor binding affinity. Hence, we concluded at this point that in the phenethanone piperazine linker phenyl region, the *p*-fluoro group appeared to be near optimal.

To evaluate in vivo antagonist activity, as a direct measure of the ability of the compound to bind and modulate the 5-HT_{2A} receptor located in the CNS, **14** was evaluated for its ability to attenuate DOI-induced hypolocomotion in rats. DOI is a potent 5-$HT_{2A/C}$ receptor agonist that crosses the blood−brain barrier. Administration of DOI in rats produces a decrease in total locomotor activity, including a suppression of rearing. This inhibition can be reversed by coadministration of a centrally acting 5-HT_{2A} antagonist/inverse agonist. For the DOI screen, test compounds were dosed orally 25 min prior to DOI (1 mg/kg subcutaneously) administration. Ten minutes after the DOI administration, animals were placed into the activity apparatus and rearing activity was measured for 10 min. Attenuation of DOI-induced hypolocomotion in rat by **14** is shown in Figure 3. As can be seen, administration of DOI 10 min before locomotor testing induced a significant decrease in rearing compared to vehicle, and this decrease was reversed in a dose-dependent fashion by pretreatment with **14**. Statistically significant reversal was observed at doses from 0.3 to

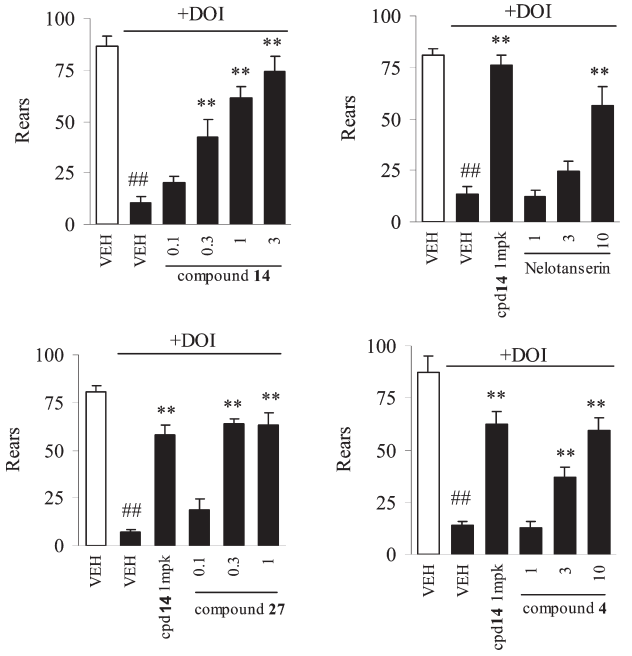

Figure 3. Attenuation of DOI-induced hypolocomotion in rat. DOI (1 mg/kg) administered 10 min prior to locomotor testing induced a decrease in locomotor activity that was reversed by 5-HT_{2A} antagonists compounds **14**, **4**, **27**, and nelotanserin: (##) $P < 0.01$ vs VEH/VEH; (**) $P < 0.01$ vs VEH/DOI; (*) $P < 0.05$ vs VEH/DOI.

Table 3. Brain and Plasma Concentration from DOI Reversal Studies in Rat[a]

compd	dose (mg/kg)	brain[b] (ng/mL)	plasma[b] (ng/mL)	B/P[b,c]
4	3	16.8	8.3	2.02
14	0.3	20.8	17.8	1.17
27	0.3	23.3	19.6	1.18
nelotanserin	3	320	488	0.65

[a] Values represent the mean of $n = 3$ animals. [b] Samples taken at the 0.75 h time point. [c] Brain to plasma ratio.

3 mg/kg. In addition brain and plasma samples were collected 45 min postdose in order to determine the brain partitioning. Compound **14** was a potent attenuator of DOI-induced hypolocomotion with an approximate ED_{50} of 0.3 mg/kg. It also showed good CNS penetration with a brain to plasma ratio of 1.17 at the ED_{50} dose (Table 3). At the 1 mg/kg dose, **14** consistently produced 75−100% of maximum reversal, and we subsequently used 1 mg/kg **14** as our internal benchmark while screening other potential compounds of interest. We considered this assay to be a useful in vivo SAR driver, as it provided a composite measure of oral absorption, brain penetration, and 5-HT_{2A} receptor antagonism.

Compound **4** was also examined in the DOI screen, on the basis of its low exposure (Table 2). It was dosed from 1 to 10 mg/kg, at 10-fold higher doses than the doses for **14**. Not surprisingly the ED_{50} was shifted by 10-fold to 3 mg/kg. However, brain and plasma sample analysis revealed that it did have a more favorable brain/plasma ratio than **14** when dosed at 3 mg/kg (Table 3).

With a view to further optimizing our lead **14**, we next turned our attention to evaluating the effect of modifications to the pyrazole moiety on receptor affinity and in vivo antagonist efficacy while maintaining the 4-fluorophenethanone piperazine linker as the molecular core. In this investigation

Scheme 2. Synthesis of Compounds **21**−**32**[a]

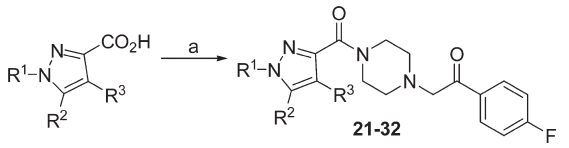

[a] Reagents and conditions: (a) 4-fluorophenethanone piperazine, HATU, Et_3N, THF or DMA.

Table 4. Binding Affinities of Compounds **21**−**32** at Human 5-HT_{2A} and 5-HT_{2C} Receptors

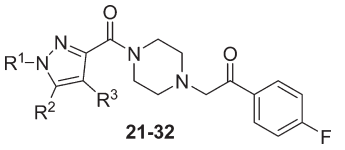

compd	R^1	R^2	R^3	5-HT_{2A} K_i[a] (nM)	5-HT_{2C} K_i[a] (nM)
14	Me	H	Br	3.9	2120
21	Me	H	H	37	1420
22	Me	Me	Br	4.6	2933
23	H	Me	Br	4.6	3573
24	H	Me	H	36	>10000
25	Me	Me	H	8.5	>10000
26	^{t}Bu	Me	H	9.3	>10000
27	Me	H	Cl	3.7	1410
28	Et	H	Cl	2.6	>10000
29	H	H	Cl	18.5	2750
30	Me	H	CF_3	28	3866
31	Me	H	I	4.5	3866
32	Ph	Me	H	11	3714

[a] K_i values are the mean of at least three experiments performed in triplicate, determined from 10 concentrations. All K_i values were calculated from IC_{50} values using the method of Cheng and Prusoff [14] with a standard deviation of < 0.4 log unit.

we examined the effects of substitutions on the pyrazole nitrogen as well as halogenation and other substitution on the pyrazole ring. The compounds were prepared from various pyrazole acids with 4-F phenethanone piperazine using *N*,*N*,*N*′,*N*′-tetramethyl-*O*-(7-azabenzotriazol-1-yl)uronium hexafluorophosphate (HATU) as the coupling agent (Scheme 2). As shown in Table 4, removal of the bromo substituent (**21**) resulted in an order of magnitude loss in 5-HT_{2A} receptor affinity. Adding an additional methyl group to the pyrazole ring (**22**) had no effect on the receptor affinity or selectivity compared to **14**. **22** also had reduced hERG binding activity (15% at 3 μM concentration). However, **22** was significantly less potent in vivo than **14** in the DOI reversal assay (65% reversal at 3 mg/kg and 22% reversal at 1 mg/kg po) most likely as a result of poorer oral absorption or brain partitioning (rat microsomes $T_{1/2} = 29$ min). If the *N*-methyl group was removed from the pyrazole moiety, the resulting compound (**23**) was again equipotent with **14** in receptor affinity. In contrast to **21**, when the bromo substituent was absent from this compound (i.e., **25**), only a modest loss of affinity for the 5-HT_{2A} receptor was observed that was accompanied by an improvement in selectivity over 5-HT_{2C}. Increasing the size of the N-substituent on the pyrazole to *tert*-butyl (**26**) or phenyl (**32**) did not further improve the 5-HT_{2A} receptor affinity.

The size of the halogen substituent had little effect on the receptor affinity; both iodo analogue **31** and chloro analogue

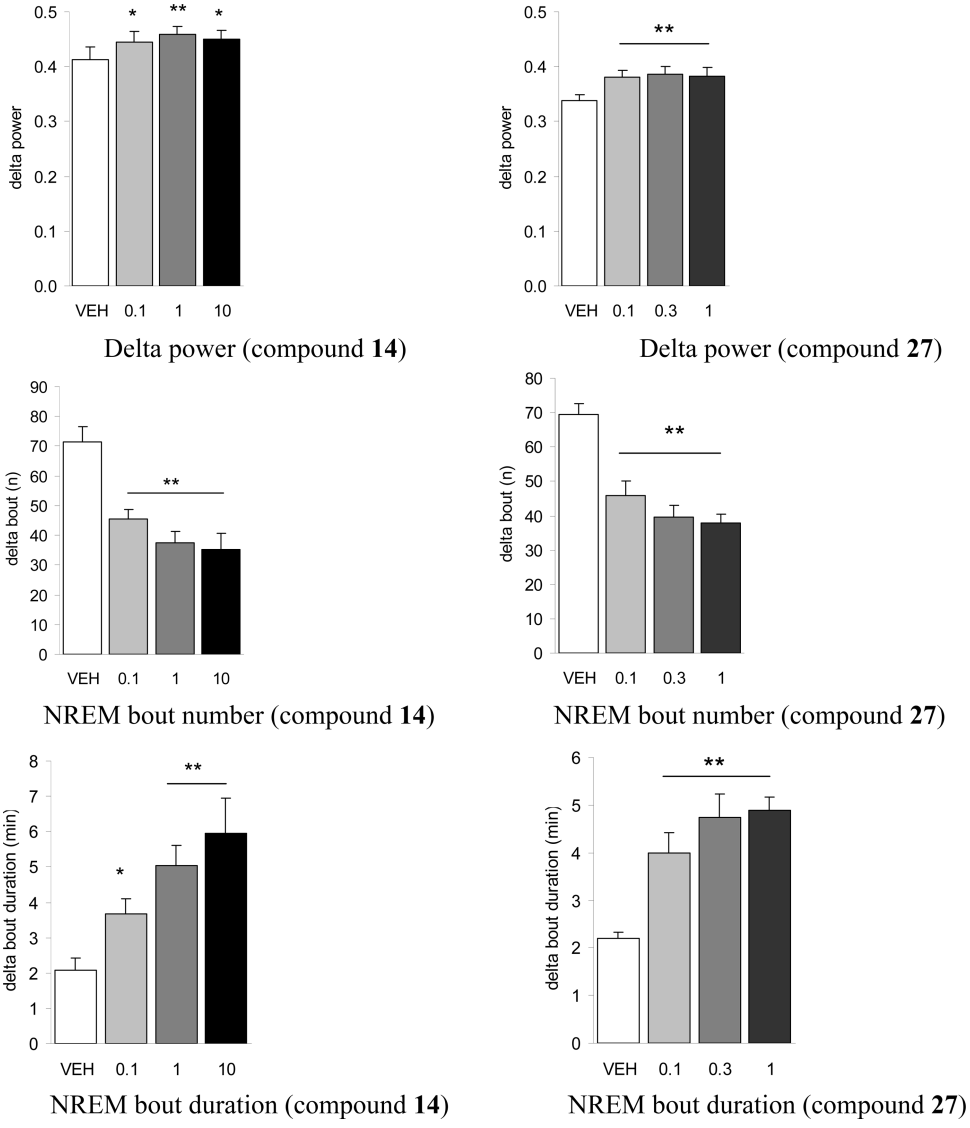

Figure 4. Rat sleep study of compounds **14** and **27**. Data represent the sum total of sleep measures recorded 5 h after compound administration. Both compounds induce a statistically significant increase in δ power (top graphs) and a dose-dependent statistically significant increase in sleep consolidation, as indicated by the concomitant decrease in NREM bout number (middle graphs) and increase in NREM bout duration (bottom graphs): (*) $P \leq 0.05$, (**) $P \leq 0.01$ vs vehicle treated controls.

27 were equipotent with the bromo analogue **14**. Replacing the *N*-methylpyrazole with *N*-ethylpyrazole (**28**) retained the 5-HT_{2A} binding affinity and appeared to be more selective on the 5-HT_{2A} receptor. Once again, however, this compound was significantly less potent than **14** in the DOI reversal assay (54% reversal at 3 mg/kg). In contrast, **27** was equipotent with **14**. At 0.3 mg/kg, **27** produced the same DOI reversal effect as **14** at 1 mg/kg. Brain and plasma sample analysis showed that it too had a good brain/plasma ratio (1.18 at 0.3 mg/kg), essentially identical to that for **14**. As a comparison, nelotanserin was dosed in the same DOI screen; as shown in Figure 3, it was about 10-fold less potent than **14** and required significantly higher brain concentration to achieve the same effect (Table 3).

In fact, **14** and **27** had the highest brain partitioning observed among the limited number of phenethanone piperazine linker derivatives that were evaluated in the DOI/CNS partitioning screen. The carbonyl group in the phenethanone piperazine linker greatly improved metabolic stability, resulting in higher exposure. It also significantly reduced hERG activity, but these improvements seemed to be at the expense of high CNS partitioning, most likely as a result of the increased polarity and H-bonding capability of the carbonyl group. Compounds **14** and **27** then appeared to represent our best compromise between the brain partitioning, oral absorption, and a range of potential off-target activities, and therefore, both compounds were selected for further profiling. Selectivity screening against a panel of 70 human GPCRs, ion channels, and transporters (Cerep) could not distinguish between the two compounds because neither showed any significant affinity (at 10 μM) for any of the targets tested, which included a wide range of monoamine receptors. CYP inhibition assays using human liver microsomes revealed that neither compound was an inhibitor of any of the major CYP isoforms (1A2, 2C9, 2C19, 2D6, and 3A4) nor was there any discernible difference in aqueous solubility, as both compounds were highly soluble. In a hERG patch clamp assay, **27** had an IC_{50} of 30 μM in a full concentration-response compared to 19 μM for **14**, which again we did not consider to be a significant difference.

On the basis of their clean in vitro profiles and good activity in the in vivo DOI reversal assay, both **14** and **27** were selected for evaluation in sleep studies. The effects of **14** on rat sleep were evaluated at doses of 0.1, 1, and 10 mg/kg. On the basis of results of this initial evaluation, **27** was evaluated at doses of 0.1, 0.3, and 1 mg/kg (Figure 4). In these studies, compounds were administered orally 6 h after lights on in the middle of the rats' inactive period (subjective night). Both δ power, which is a measure of deep sleep, and sleep consolidation were analyzed. Both **14** and **27** significantly increased δ power 1 h after dosing at 0.1 mg/kg compared to vehicle treated controls, and the effect lasted 3−4 h following dosing. Although these effects lacked a clear dose-dependence, significant effects on δ sleep were observed at the lowest dose (0.1 mg/kg) tested. Both compounds significantly and dose-dependently increased sleep consolidation, as indicated by the decrease in nonrapid eye movement (NREM) bout number and increase in NREM bout duration. The minimum effective dose for increasing sleep consolidation was 0.1 mg/kg for both compounds.

Since **14** and **27** were almost identical in most aspects of the in vitro profile and they both significantly improved deep sleep and sleep consolidation at 0.1 mg/kg, we chose **27** for further evaluation solely on the basis of our in-house preference to avoid bromo substituents in clinical candidates where at all possible. Although no safety or stability issues had been observed, as all other parameters were comparable, we judged the chloro derivative to hold a lower risk in development.

We profiled **27** more widely across cloned 5-HT_{2A} receptors from other species. In all cases, the binding affinity for the different receptors was similar to that for the human receptor (Table 5). In addition, **27** showed low plasma protein binding in human, rat, dog, and monkey with free fractions ranging from 29% to 49% (Table 5).

The pharmacokinetic properties of **27** across several preclinical species were also examined (Table 6). The iv pharmacokinetics of **27** exhibited low (dog and monkey) to moderate (mouse and rat) clearance rates and low volumes of distribution. Upon oral administration at 3 mg/kg, **27** was quickly absorbed, overall exposure was high, and oral bioavailability was good in monkey and excellent in mouse, rat, and dog. In addition, a dose escalating PK study in rat showed that **27** displayed dose-linear increases in both overall exposure and C_{max} in the range of 0.3−300 mg/kg.

Compound **27** was well tolerated acutely in mouse and rat at doses up to 300 mg/kg. Some reduction in locomotor activity was seen at 300 mg/kg and higher, and this locomotor impairment was confirmed in the rotarod test at the same dose. No adverse effects on hemodynamic or ECG parameters were observed after acute doses of up to 10 and 30 mg/kg in telemeterized rats and dogs, respectively.

A salt screening of around 10 potential counterions identified the hydrochloride salt of **27** as a potential salt for further development. The HCl salt of **27** was highly crystalline, only moderately hygroscopic (< 2% water adsorption at >80% RH) with a high melting point (~204 °C) and showed only a single crystalline form after slurrying in multiple solvents.

In summary, a series of phenethylpiperazine amides were synthesized. Introduction of a carbonyl group to the phenethylpiperazine linker improved metabolic stability and reduced hERG activity but resulted in decreased CNS partitioning. We were able to identify compounds with potent receptor affinity, high selectivity, and favorable brain penetration that had good pharmacokinetic properties and an acceptable early safety profile. Rat sleep studies using **14** and **27** demonstrated that both were efficacious at inducing sleep consolidation and increasing deep sleep at 0.1 mg/kg. Although there were no discernible differences in the overall profiles, we selected the hydrochloride salt of **27** for further development on the basis of our belief that the analogue with a chloro substituent was preferable to that with a bromo substituent to avoid potential downstream risks. We believe that **27** provides the opportunity for further investigation of 5-HT_{2A} inverse agonists as potential therapeutics for the treatment of insomnia.

Table 5. 5-HT_{2A} Receptor Binding Affinity and Plasma Protein Binding of **27** in Different Species

species	human	monkey	dog	rat
5-HT_{2A} K_i (nM)	3.6	1.7	2.7	2.4
plasma protein binding[a]	69	71	61	51

[a] % bound.

Experimental Section

Chemistry. All reagents were commercially available and used without further purification unless stated otherwise. Microwave irradiations were performed using either a Smith Synthesizer or an Emrys Optimizer (Biotage). Column chromatography was carried out on prepacked silica gel columns using KP-Sil supplied by Biotage and on silica gel column using Kieselgel 60, 0.063−0.200 mm (Merck). Proton nuclear magnetic resonance (^{1}H NMR) spectra were recorded on a Bruker Avance-400 equipped with a quad nucleus probe (QNP) or a broadband inverse (BBI) probe and *z*-gradient. Chemical shifts (δ) are given in parts per million (ppm) with the residual solvent signal used as a reference. Coupling constants (*J*) are reported in Hz. NMR abbreviations are used as follows: s = singlet, d = doublet, t = triplet, q = quartet, m = multiplet, dd = doublet of doublets, dt = doublet of triplets, b = broad, bs = broad singlet. Melting points were recorded on differential scanning calorimetry (DSC).

Analytical HPLC/MS was conducted on a PE Sciex API 150EX mass spectrometer with an electrospray source, using a Shimadzu Inc. LC-10A VP UV detector monitoring at 214 nm, Analyst 1.2 software, and either (a) a Gilson 215 autosampler and an Alltech Prevail C18 column (5 μm, 250 mm × 4.6 mm), using a gradient of 5% v/v CH_3CN (containing 1% v/v TFA) in H_2O (containing 1% v/v TFA) (t = 0.0 min) gradient to 95% v/v CH_3CN in H_2O (t = 6.0 min), 3.5 mL/min or (b) a PE 200 autosampler and a Supelco Discovery C18 column (5 μm,

Table 6. Pharmacokinetic Profile of **27** in Preclinical Species after 3 mg/kg Oral Dose[a]

species	C_{max} (ng/mL)	AUC_{last} (h·ng/mL)	$T_{1/2}$ (h)	IV CL_{total} ((L/h)/kg)	V_{ss} (L/kg)	F (%)[b]
mouse	718	459	0.5	5.6	1.7	87
rat	1043[c]	1185[c]	2.0	5.6	1.7	67
dog	1255	2941	5.2	0.9	1.9	94
monkey	600	872	0.6	0.9	0.4	26

[a] Values represent the mean of n = 3 animals. [b] F calculated relative to a 2 mg/kg iv dose. [c] Values from 10 mg/kg oral dose.

50 mm × 2.1 mm), using a gradient of 5% v/v CH_3CN (containing 1% v/v TFA) in H_2O (containing 1% v/v TFA) (t = 0.0 min) gradient to 95% v/v CH_3CN in H_2O (t = 5.0 min), 0.75 mL/min. Preparative HPLC was conducted on a Varian Prostar reverse phase HPLC using either (a) a Phenomenex Luna C18 column (10 μm, 250 mm × 21.2 mm), 5% (v/v) CH_3CN (containing 0.1% v/v TFA) in H_2O (containing 0.1% v/v TFA) gradient to 95% CH_3CN, 20 mL/min, λ = 220 nm or (b) a Phenomenex Luna C18 column (10 μm, 250 mm × 50 mm), 5% (v/v) CH_3CN (containing 0.1% v/v TFA) in H_2O (containing 0.1% v/v TFA) gradient to 95% CH_3CN, 50 mL/min, λ = 220 nm. Purity of the tested compounds was ≥95% based on LCMS data unless stated otherwise.

***N*-[3-(4-Chloro-1-methyl-1*H*-pyrazol-5-yl)-4-methoxyphenyl]-4-(4-fluorophenethyl)piperazine-1-carboxamide (2).** 3-(4-Chloro-1-methyl-1*H*-pyrazol-5-yl)-4-methoxyaniline (237 mg, 1 mol) was added to a solution of 1-(4-fluorophenethyl)piperazine (312 mg, 1.5 mol), 1,1′-carbonyldiimidazole (243 mg, 1.5 mol), and triethylamine (417 μL, 3 mol) in THF (2 mL). The reaction mixture was heated to 100 °C for 20 min in the microwave. The solvent was removed under reduced pressure and the residue was purified by HPLC to afford the TFA salt of **2** (441 mg, 94%) as a white solid. ^{1}H NMR ($CDCl_3$, 400 MHz) δ 2.82−3.10 (m, 4H), 3.11−3.22 (m, 4H), 3.55−3.65 (m, 2H), 3.62 (s, 3H), 3.81 (s, 3H), 4.30 (bs, 2H), 6.93−6.95 (m, 1H), 6.99−7.04 (m, 2H), 7.15−7.19 (m, 2H), 7.28−7.30 (m, 1H), 7.42 (s, 1H), 7.50 (s, 1H), 7.48−7.52 (m, 1H). LCMS m/z = 472.3/473.2 $[M + H]^+$.

***N*-(4-Bromo-1*H*-pyrazol-3-yl)-4-(4-fluorophenethyl)piperazine-1-carboxamide (3).** 4-Bromo-1*H*-pyrazol-3-amine (145 mg, 0.89 mmol) was added to a solution of 1-(4-fluorophenethyl)piperazine (62 mg, 0.3 mmol), 1,1′-carbonyldiimidazole (145 mg, 0.9 mmol), and triethylamine (123 μL, 0.9 mmol) in DMSO (1.5 mL). The reaction mixture was heated to 100 °C for 20 min in the microwave. The crude mixture was purified by HPLC to afford the TFA salt of **3** (28 mg, 21% yield, 90% pure) as a white solid. ^{1}H NMR (CD_3CN, 400 MHz) δ 3.00−3.10 (m, 2H), 3.23−3.32 (m, 2H), 3.41−3.63 (m, 4H), 4.00 (bs, 2H), 4.73 (bs, 2H), 7.07−7.11 (m, 2H), 7.27−7.31 (m, 2H), 8.02 (s, 1H). LCMS m/z = 396.2/398.2 $[M + H]^+$.

General Procedure A: Preparation of (4-Bromo-1-methyl-1*H*-pyrazol-3-yl)-{4-[2-(4-fluorophenyl)ethyl]piperazin-1-yl}methanone (4). A mixture of 1-(4-fluorophenethyl)piperazine (68 mg, 0.33 mmol), 4-bromo-1-methyl-1*H*-pyrazole-3-carboxylic acid (87 mg, 0.42 mmol), *O*-(7-azabenzotriazol-1-yl)-*N*,*N*,*N*′,*N*′-tetramethyluronium hexafluorophosphate (HATU, 161 mg, 0.42 mmol), and triethylamine (0.1 mL) in THF (1 mL) was heated in microwave at 100 °C for 10 min. The crude mixture was purified by HPLC to afford the TFA salt of **4** (111 mg, 86%) as a white solid. ^{1}H NMR (acetonitrile-d_3, 400 MHz) δ 3.01−3.09 (m, 4H), 3.27−3.33 (m, 2H), 3.48−3.74 (m, 4H), 3.86 (s, 3H), 4.29−4.42 (m, 1H), 4.63−4.73 (m, 1H), 7.09 (t, J = 8.8 Hz, 2H), 7.29 (dd, J = 5.1, 8.8 Hz, 2H), 7.67 (s, 1H) . LCMS m/z = 395.3/397.3 $[M + H]^+$.

(4-Bromo-1-methyl-1*H*-pyrazol-3-yl)-(4-phenethylpiperazin-1-yl)methanone (5). 5 was prepared in a manner similar to that described for **4** using (2-bromoethyl)benzene (50 mg, 0.26 mmol) and 4-bromo-1-methyl-1*H*-pyrazole-3-carboxylic acid (65 mg, 0.32 mmol) and was obtained as an off-white solid (51 mg, 52%). ^{1}H NMR (DMSO-d_6, 400 MHz) δ 2.91−3.02 (m, 2H), 3.02−3.30 (m, 4H), 3.36−3.80 (m, 4H), 3.88 (s, 3H), 4.21−4.34 (m, 1H), 4.51−4.62 (m, 1H), 7.25−7.31 (m, 3H), 7.33−7.38 (m, 2H), 8.10 (s, 1H). LCMS m/z = 377.4/379.4 $[M + H]^+$.

(4-Bromo-1-methyl-1*H*-pyrazol-3-yl)piperazin-1-ylmethanone (6). Step 1: *tert*-Butyl 4-(4-Bromo-1-methyl-1*H*-pyrazole-3-carbonyl)piperazine-1-carboxylate. A mixture of 4-bromo-1-methyl-1*H*-pyrazole-3-carboxylic acid (500 mg, 2.44 mmol), 1-*N*-Boc-piperazine (454 mg, 2.44 mmol), HATU (1.11 g, 2.92 mmol), and triethylamine (1.0 mL) in THF (3 mL) was heated in microwave at 100 °C for 5 min. The crude mixture was purified by HPLC to afford the TFA salt of the title compound (820 mg, 90%) as an off-white solid. ^{1}H NMR (acetonitrile-d_3, 400 MHz) δ 1.49 (s, 9H), 3.43−3.46 (m, 2H), 3.50−3.53 (m, 4H), 3.68−3.70 (m, 2H), 3.91 (s, 3H), 7.69 (s, 1H). LCMS m/z = 373.1/375.1$[M + H]^+$.

Step 2. The intermediate from step 1 above (800 mg, 2.14 mmol) and HCl in dioxane (4 N, 5.36 mL) were stirred at room temperature for 1 h. The solvent was removed under reduced pressure to afford **6** as a hydrochloride salt (585 mg, 89%) as a light-yellow solid. ^{1}H NMR (acetonitrile-d_3, 400 MHz) δ 3.20−3.26 (m, 4H), 3.92 (s, 3H), 3.98−4.05 (m, 4H), 7.71 (s, 1H), 9.40−9.50 (bs, 2H). LCMS m/z = 273.0/275.0 $[M + H]^+$.

General Procedure B: Preparation of (4-Bromo-1-methyl-1*H*-pyrazol-3-yl)-{4-[2-(2-fluorophenyl)ethyl]piperazin-1-yl}methanone (7). A mixture of **6** (40.0 mg, 0.15 mmol), 1-(2-bromoethyl)-2-fluorobenzene (31 μL, 0.22 mmol), and potassium carbonate (60.7 mg, 0.45 mmol) in acetonitrile (2 mL) was heated at 150 °C for 20 min under microwave irradiation in a heavy-walled sealed tube. Excess potassium carbonate was removed by filtration and the filtrate was purified by HPLC to afford the TFA salt of **7** (17 mg, 29%) as a white solid. ^{1}H NMR (DMSO-d_6, 400 MHz) δ 3.02−3.15 (m, 8H), 3.88 (s, 3H), 4.20−4.30 (m, 2H), 4.51−4.61 (m, 2H), 7.19−7.24 (m, 2H), 7.33−7.38 (m, 2H), 8.09 (s, 1H), 9.94 (s, 1H). LCMS m/z = 395.4/397.4 $[M + H]^+$.

(4-Bromo-1-methyl-1*H*-pyrazol-3-yl)-{4-[2-(3-fluorophenyl)ethyl]-piperazin-1-yl}methanone (8). 8 was prepared in a manner similar to that described for **7** using 1-(2-bromoethyl)-3-fluorobenzene (35.7 mg, 0.176 mmol) and **6** (40 mg, 0.146 mmol) and was obtained as a white solid (13 mg, 15%). ^{1}H NMR (DMSO-d_6, 400 MHz) δ 3.01−3.26 (m, 6H), 3.36−3.70 (m, 4H), 3.88 (s, 3H), 4.25 (bs, 1H), 4.58 (bs, 1H), 7.08−7.18 (m, 3H), 7.36−7.43 (m, 1H), 8.08 (s, 1H), 10.1 (s, 1H). LCMS m/z = 395.2/397.2 $[M + H]^+$.

(4-Bromo-1-methyl-1*H*-pyrazol-3-yl)-{4-[2-(4-chlorophenyl)-ethyl]piperazin-1-yl}methanone (9). 9 was prepared in a manner similar to that described for **7** using 1-(2-bromoethyl)-4-chlorobenzene (26 μL, 0.18 mmol) and **6** (40 mg, 0.146 mmol) and was obtained as a white solid (8 mg, 13%). ^{1}H NMR (CD_3CN, 400 MHz) δ 2.73 (bs, 6H), 3.11−3.19 (m, 2H), 3.27−3.41 (m, 4H), 3.92 (s, 3H), 7.30−7.34 (m, 2H), 7.39−7.43 (m, 2H), 7.72 (s, 1H). LCMS m/z = 411.2/413.2 $[M + H]^+$.

(4-Bromo-1-methyl-1*H*-pyrazol-3-yl)-{4-[2-(4-methoxyphenyl)-ethyl]piperazin-1-yl}methanone (10). 10 was prepared in a manner similar to that described for **7** using 1-(2-bromoethyl)-4-methoxybenzene (35 mg, 0.165 mmol) and **6** (46 mg, 0.15 mmol) and was obtained as a white solid (45 mg, 74%). ^{1}H NMR (acetonitrile-d_3, 400 MHz) δ 3.05−3.07 (m, 4H), 3.30−3.35 (m, 4H), 3.55−3.66 (m, 4H), 3.82 (s, 3H), 3.92 (s, 3H), 6.94−6.97 (m, 2H), 7.22−7.26 (m, 2H), 7.72 (s, 1H). LCMS m/z = 407.4/409.4 $[M + H]^+$.

(4-Bromo-1-methyl-1*H*-pyrazol-3-yl)-{4-[2-(2,4-difluorophenyl)-ethyl]piperazin-1-yl}methanone (11). Step 1: *tert*-Butyl 4-[2-(2,4-Difluorophenyl)acetyl]piperazine-1-carboxylate. 2-(2,4-Difluorophenyl)acetic acid (5.00 g, 29.1 mmol), 1*H*-benzo[*d*][1,2,3]triazol-1-ol (4.46 g, 29.1 mmol), *N*-ethyl-*N*′-(3-dimethylaminopropyl)-carbodiimide hydrochloride (5.57 g, 29.1 mmol), and triethylamine (4.05 mL, 29.1 mmol) were stirred in 1,2-dichloromethane (30 mL) for 15 min. *tert*-Butyl piperazine-1-carboxylate (2.71 g, 14.5 mmol) was added, and the mixture was stirred at room temperature for 8 h. The reaction mixture was diluted with 1,2-dichloromethane (10 mL) and washed with 1 N NaOH (5 mL), followed by 1 M citric acid (5 mL). The organic portion was dried over Na_2SO_4, filtered, concentrated, and purified by HPLC. The product-containing fractions were lyophilized to afford material that was neutralized with saturated $NaHCO_3$ (75 mL) and extracted with EtOAc (2 × 200 mL). The organic extracts were dried over Na_2SO_4, filtered, and concentrated to afford the title compound (1.68 g, 34%) as a yellow solid. ^{1}H NMR (DMSO-d_6, 400 MHz) δ 1.42 (s, 9H), 3.25−3.39 (m, 4H), 3.42−3.48 (m, 2H), 3.49−3.56 (m, 2H), 3.74 (s, 2H), 7.02 (dt, J = 2.7, 8.5 Hz, 1H), 7.18 (dt, J = 2.6, 9.7 Hz, 1H), 7.25−7.33 (m, 1H). LCMS m/z = 341.3 $[M + H]^+$.

Step 2: *tert*-Butyl 4-(2,4-Difluorophenethyl)piperazine-1-carboxylate. The intermediate from step 1 (1.12 g, 3.30 mmol) was dissolved in THF (8.5 mL), and borane−tetrahydrofuran complex (1.0 M, 15.8 mL, 15.8 mmol) was added. The mixture was heated under reflux for 2 h. The reaction was slowly quenched by dropwise addition of methanol (0.4 mL). Then 0.5 M HCl (10.0 mL) was added, and the mixture was extracted with EtOAc (2 × 100 mL). The combined organic extracts were dried over Na_2SO_4, filtered, and concentrated to give a residue that was purified by HPLC. The combined product containing fractions were added to saturated $NaHCO_3$ (20 mL) and extracted with EtOAc (2 × 100 mL). The organic extracts were dried over Na_2SO_4, filtered, and concentrated to yield the title compound (1.08 g, 98%) as a white solid. ^{1}H NMR (DMSO-d_6, 400 MHz) δ 1.41 (s, 9H), 2.80−2.96 (m, 6H), 3.10−3.03 (m, 2H), 3.50−3.60 (m, 4H), 7.06 (dt, J = 2.6, 8.5 Hz, 1H), 7.22 (dt, J = 2.6, 9.6 Hz, 1H), 7.38−7.46 (m, 1H). LCMS m/z = 327.1 $[M + H]^+$.

Step 3: 1-(2,4-Difluorophenethyl)piperazine. The intermediate from step 2 (0.853 g, 2.61 mmol) was dissolved in 4 M HCl in dioxane (10.0 mL) and stirred for 1 h. The mixture was concentrated to afford the dihydrochloride salt of the title compound (0.718 g, 92%) as a pale-yellow solid. ^{1}H NMR (DMSO-d_6, 400 MHz) δ 2.95−3.75 (m, 12H), 6.03−6.80 (bs, 1H), 7.04−7.12 (m, 1H), 7.24 (dt, J = 2.6, 9.6 Hz, 1H), 7.39−7.50 (m, 1H). LCMS m/z = 227.2 $[M + H]^+$.

Step 4: (4-Bromo-1-methyl-1*H*-pyrazol-3-yl)-{4-[2-(2,4-difluorophenyl)ethyl]piperazin-1-yl}methanone (11). 11 was prepared in a manner similar to that described for **4** using the intermediate from step 3 (15 mg, 0.064 mmol) and **6** (20 mg, 0.058 mmol) and was obtained as a yellow solid (15 mg, 62%). ^{1}H NMR (DMSO-d_6, 400 MHz) δ 2.90−3.80 (m, 10H), 3.87 (s, 3H), 4.18−4.40 (bs, 1H), 4.45−4.69 (bs, 1H), 7.07−7.16 (m, 1H), 7.23−7.33 (m, 1H), 7.39−7.47 (m, 1H), 8.09 (s, 1H). LCMS m/z = 413.1/415.1 $[M + H]^+$.

3-{2-[4-(4-Bromo-1-methyl-1*H*-pyrazole-3-carbonyl)piperazin-1-yl]ethyl}-2-methyl-6,7,8,9-tetrahydro-4*H*-pyrido[1,2-*a*]pyrimidin-4-one (12). 12 was prepared in a manner similar to that described for **7** using 3-(2-chloroethyl)-2-methyl-6,7,8,9-tetrahydro-4*H*-pyrido[1,2-*a*]pyrimidin-4-one (37 mg, 0.165 mmol) and **6** (46 mg, 0.15 mmol) and was obtained as a solid (69 mg, 99%). ^{1}H NMR (acetonitrile-d_3, 400 MHz) δ 1.90−1.94 (m, 2H), 1.99−2.06 (m, 6H), 2.42 (s, 3H), 2.97−3.11 (m, 6H), 3.26−3.30 (m, 4H), 3.91−3.94 (m, 2H), 3.93 (s, 3H), 7.73 (s, 1H). LCMS m/z = 463.4/465.4 $[M + H]^+$.

2-{2-[4-(4-Bromo-1-methyl-1*H*-pyrazole-3-carbonyl)piperazin-1-yl]ethyl}isoindoline-1,3-dione (13). 13 was prepared in a manner similar to that described for **7** using 2-(2-bromoethyl)isoindoline-1,3-dione (42 mg, 0.165 mmol) and **6** (46 mg, 0.15 mmol) and was obtained as a solid (14 mg, 21%). ^{1}H NMR (acetonitrile-d_3, 400 MHz) δ 3.47−3.50 (m, 8H), 3.92 (s, 3H), 3.90−3.95 (m, 2H), 4.06−4.09 (m, 2H), 7.72 (s, 1H), 7.83−7.90 (m, 4H). LCMS m/z = 446.5/448.5 $[M + H]^+$.

2-[4-(4-Bromo-1-methyl-1*H*-pyrazole-3-carbonyl)piperazin-1-yl]-1-(4-fluorophenyl)ethanone (14). Step 1: *tert*-Butyl 4-[2-(4-Fluorophenyl)-2-oxoethyl]piperazine-1-carboxylate. *tert*-Butyl piperazine-1-carboxylate (5.00 g, 26.8 mmol) was dissolved in DMF (15 mL). 2-Bromo-1-(4-fluorophenyl)ethanone (7.00 g, 32.2 mmol) and potassium carbonate (11.1 g, 80.5 mmol) were then added to the solution. The reaction mixture was stirred at room temperature for 10 min. The crude product was purified by HPLC to afford the TFA salt of the title compound (9.06 g, 96%) as a pale-yellow oil. ^{1}H NMR (acetonitrile-d_3, 400 MHz) δ 1.47 (s, 9H), 3.37 (bs, 4H), 3.78 (bs, 4H), 4.75−4.76 (m, 2H), 7.31−7.35 (m, 2H), 8.02−8.05 (m, 2H). LCMS m/z = 323.2 $[M + H]^+$.

Step 2: 1-(4-Fluorophenyl)-2-(piperazin-1-yl)ethanone. The product from step 1 (8.65 g, 26.8 mmol) in dioxane (5 mL) was treated with 4 M HCl in dioxane (20 mL) and the mixture stirred at 43 °C for 1 h. The solvent was removed under reduced pressure and the residue was dried in a vacuum oven to yield the title compound (5.29 g, 88%) as a white solid. LCMS m/z = 223.4 $[M + H]^+$. The product was used without further purification.

Step 3: 2-[4-(4-Bromo-1-methyl-1*H*-pyrazole-3-carbonyl)piperazin-1-yl]-1-(4-fluorophenyl)ethanone (14). 14 was prepared in a manner similar to that described for **4** using the intermediate from step 2 (1 g, 3.38 mmol) and 4-bromo-1-methyl-1*H*-pyrazole-3-carboxylic acid (693 mg, 3.38 mmol) and was obtained as a white solid (1.5 g, 85%). Preparation of oxalate salt was as follows: **14** (6 g, 14.6 mmol) was dissolved in ethanol (50 mL), and oxalic acid (1.32 g, 14.6 mmol) was added. The resulting slurry was heated to 50 °C to give a semiclear solution which was then cooled to room temperature overnight. The solid was filtered off and dried to afford **14** oxalate salt (5.75 g), mp 197 °C. ^{1}H NMR (DMSO-d_6, 400 MHz) δ 3.07−3.33 (m, 2H), 3.50−3.80 (m, 4H), 3.87 (s, 3H), 4.07−4.28 (m, 1H), 4.35−4.55 (m, 1H), 4.94−5.18 (m, 2H), 7.48 (t, J = 8.7 Hz, 2H), 8.04−8.11 (m, 3H). LCMS m/z = 409.4/411.4 $[M + H]^+$.

2-[4-(4-Bromo-1-methyl-1*H*-pyrazole-3-carbonyl)piperazin-1-yl]-1-(2,4-difluorophenyl)ethanone (15). 15 was prepared in a manner similar to that described for **7** using 2-bromo-1-(2,4-difluorophenyl)ethanone and **6** (46 mg, 0.15 mmol) and was obtained as a white solid (36 mg, 59%). ^{1}H NMR (acetonitrile-d_3, 400 MHz) δ 3.41−3.52 (m, 4H), 3.92 (s, 3H), 4.02−4.15 (m, 4H), 4.68 (d, J = 2.8 Hz, 2H), 7.18−7.25 (m, 2H), 7.73 (s, 1H), 8.08−8.14 (m, 1H). LCMS m/z = 427.2/429.2 $[M + H]^+$.

2-[4-(4-Bromo-1-methyl-1*H*-pyrazole-3-carbonyl)piperazin-1-yl]-1-(2-fluorophenyl)ethanone (16). 16 was prepared in a manner similar to that described for **7** using 2-bromo-1-(2-fluorophenyl)ethanone (26 mg, 0.12 mmol) and **6** (31 mg, 0.1 mmol) and was obtained as a white solid (6 mg, 15%). ^{1}H NMR (DMSO-d_6, 400 MHz) δ 2.80−3.75 (m, 8H), 3.87 (s, 3H), 4.00−4.60 (m, 1H), 4.70−5.11 (bs, 1H), 7.30−7.51 (m, 2H), 7.68−7.85 (m, 1H), 7.86−8.02 (m, 1H), 8.07 (s, 1H). LCMS m/z = 409.4/411.4 $[M + H]^+$.

2-[4-(4-Bromo-1-methyl-1*H*-pyrazole-3-carbonyl)piperazin-1-yl]-1-(4-trifluoromethylphenyl)ethanone (17). 17 was prepared in a manner similar to that described for **7** using 2-bromo-1-[4-(trifluoromethyl)phenyl]ethanone (65 mg, 0.24 mmol) and **6** (75 mg, 0.24 mmol) and was obtained as a white solid (47 mg, 42%). ^{1}H NMR (methanol-d_4, 400 MHz) δ 3.47−3.56 (m, 4H), 3.93 (s, 3H), 4.04−4.16 (m, 4H), 5.08 (s, 2H), 7.85 (s, 1H), 7.92 (d, J = 8.3 Hz, 2H), 8.22 (d, J = 8.3 Hz, 2H). LCMS m/z = 459.3/461.3 $[M + H]^+$.

2-[4-(4-Bromo-1-methyl-1*H*-pyrazole-3-carbonyl)piperazin-1-yl]-1-(4-trifluoromethoxyphenyl)ethanone (18). 18 was prepared in a manner similar to that described for **7** using 2-bromo-1-[4-(trifluoromethoxy)phenyl]ethanone (68 mg, 0.24 mmol) and **6** (75 mg, 0.24 mmol) and was obtained as a white solid (68 mg, 60%). ^{1}H NMR (methanol-d_4, 400 MHz) δ 3.46−3.56 (m, 4H), 3.93 (s, 3H), 4.04−4.18 (m, 4H), 5.04 (s, 2H), 7.50 (d, J = 8.8 Hz, 2H), 7.85 (s, 1H), 8.16 (d, J = 8.8 Hz, 2H). LCMS m/z = 475.4/477.4 $[M + H]^+$.

(4-Bromo-1-methyl-1*H*-pyrazol-3-yl)-{4-[2-(4-fluorophenyl)-2-hydroxyethyl]piperazin-1-yl}methanone (19). 14 (30 mg, 0.070 mmol) was taken up in MeOH (4 mL), the solution cooled to 0 °C, and sodium borohydride (3 mg, 0.070 mmol) added. The reaction mixture was stirred at room temperature for 5 min and then quenched with water. The solvent was removed under reduced pressure and the crude product purified by HPLC to afford the TFA salt of **19** (25 mg, 83%) as a white solid. ^{1}H NMR (acetonitrile-d_3, 400 MHz) δ 2.92−4.16 (m, 8H), 3.23−3.29 (m, 2H), 3.87 (s, 3H), 5.15−5.20 (m, 1H), 7.14 (t, J = 8.8 Hz, 2H), 7.44 (dd, J = 5.3, 8.8 Hz, 2H), 7.67 (s, 1H). LCMS m/z = 411.2/413.2 $[M + H]^+$.

2-[4-(4-Bromo-1-methyl-1*H*-pyrazole-3-carbonyl)piperazin-1-yl]-1-(4-fluorophenyl)ethanone *O*-Methyloxime (20). 14 (100 mg, 0.24 mmol) and methoxylamine hydrochloride (25 mg, 0.31 mmol) were dissolved in ethanol (10 mL) in a round-bottom flask and heated to reflux at 90 °C for 21 h. The solvent was removed under reduced pressure, and saturated $NaHCO_3$ (2 mL) was

added. The mixture was extracted three times with 1,2-dichloromethane, and the combined organic phases were dried over sodium sulfate, filtered, and concentrated. The crude product was purified by preparative TLC (R_f = 0.44, 60% EtOAc/hexane, UV 254 nm) to afford **20** (67 mg, 63%) as a white solid. ^{1}H NMR (acetonitrile-d_3, 400 MHz) δ 2.42−2.48 (m, 2H), 2.48−2.54 (m, 2H), 3.35−3.42 (m, 2H), 3.37 (s, 2H), 3.57−3.63 (m, 2H), 3.80 (s, 3H), 3.84 (s, 3H), 7.14 (t, J = 8.8 Hz, 2H), 7.60 (dd, J = 5.3, 8.8 Hz, 2H), 7.61 (s, 1H). LCMS m/z = 438.3/440.3 $[M + H]^+$.

1-(4-Fluorophenyl)-2-[4-(1-methyl-1*H*-pyrazole-3-carbonyl)-piperazin-1-yl]ethanone (21). 21 was prepared in a manner similar to that described for **14** using 1-methyl-1*H*-pyrazole-3-carboxylic acid (25.0 mg, 0.20 mmol) and 1-(4-fluorophenyl)-2-(piperazin-1-yl)ethanone dihydrochloride (64 mg, 0.22 mmol) and was obtained as a white solid (40 mg, 61%). ^{1}H NMR (DMSO-d_6, 400 MHz) δ 3.24 (bs, 2H), 3.40−3.62 (bs, 3H), 3.78−3.88 (bs, 1H), 3.89 (s, 3H), 4.50 (bs, 1H), 4.90 (bs, 1H), 5.09 (s, 2H), 6.64 (d, J = 2.3 Hz, 1H), 7.49 (t, J = 8.8 Hz, 2H), 7.80 (d, J = 2.3 Hz, 1H), 8.06−8.11 (m, 2H), 10.4 (bs, 1H). LCMS m/z = 331.4 $[M + H]^+$.

2-[4-(4-Bromo-1,5-dimethyl-1*H*-pyrazole-3-carbonyl)piperazin-1-yl]-1-(4-fluorophenyl)ethanone (22). 22 was prepared using **25** (194 mg, 0.560 mmol) and NBS (120 mg, 0.680 mmol) as starting materials and was obtained as the TFA salt (51 mg, 22%) as a white solid. ^{1}H NMR (acetonitrile-d_3, 400 MHz) δ 2.27 (s, 3H), 3.30−3.53 (m, 4H), 3.79 (s, 3H), 3.78−4.28 (m, 2H), 4.46−5.05 (m, 2H), 4.77 (s, 2H), 7.32 (t, J = 8.8 Hz, 2H), 8.02 (dd, J = 5.3, 8.8 Hz, 2H). LCMS m/z = 423.3/425.3 $[M + H]^+$.

2-[4-(4-Bromo-5-methyl-1*H*-pyrazole-3-carbonyl)piperazin-1-yl]-1-(4-fluorophenyl)ethanone (23). 23 was prepared using **24** (80 mg, 0.24 mmol) and NBS (116 mg, 0.65 mmol) as starting materials and was obtained as the TFA salt (11 mg, 11%) as a white solid. ^{1}H NMR (acetonitrile-d_3, 400 MHz) δ 2.26 (s, 3H), 3.33−3.52 (m, 4H), 3.93−4.12 (m, 4H), 4.74 (s, 2H), 7.30 (t, J = 8.8 Hz, 2H), 8.01 (dd, J = 5.3, 8.8 Hz, 2H). LCMS m/z = 409.3/411.3 $[M + H]^+$.

1-(4-Fluorophenyl)-2-[4-(5-methyl-2*H*-pyrazole-3-carbonyl)-piperazin-1-yl]ethanone (24). 24 was prepared in a manner similar to that described for **14** using 3-methyl-1*H*-pyrazole-5-carboxylic acid (19 mg, 0.15 mmol) and 1-(4-fluorophenyl)-2-(piperazin-1-yl)ethanone dihydrochloride (49 mg, 0.165 mmol) and was obtained as a solid (26 mg, 53%). ^{1}H NMR (400 MHz, $CDCl_3$) δ 2.34 (s, 3H), 2.66 (bs, 4H), 3.82 (s, 2H), 3.88 (bs, 2H), 4.02 (bs, 2H), 6.38 (s, 1H), 7.14 (t, J = 8.6 Hz, 2H), 7.99−8.09 (m, 2H). LCMS m/z = 331.3 $[M + H]^+$.

2-[4-(1,5-Dimethyl-1*H*-pyrazole-3-carbonyl)piperazin-1-yl]-1-(4-fluorophenyl)ethanone (25). 25 was prepared in a manner similar to that described for **14** using 1,5-dimethyl-1*H*-pyrazole-3-carboxylic acid (182 mg, 1.30 mmol) and 1-(4-fluorophenyl)-2-(piperazin-1-yl)ethanone dihydrochloride (422 mg, 1.43 mmol) and was obtained as a white solid (411 mg, 91%). ^{1}H NMR (acetonitrile-d_3, 400 MHz) δ 2.27 (s, 3H), 3.19−3.58 (m, 4H), 3.76 (s, 3H), 3.84−4.17 (m, 4H), 4.76 (s, 2H), 6.43 (s, 1H), 7.32 (t, J = 8.8 Hz, 2H), 8.02 (dd, J = 5.3, 8.8 Hz, 2H). LCMS m/z = 345.4 $[M + H]^+$.

2-[4-(1-*tert*-Butyl-5-methyl-1*H*-pyrazole-3-carbonyl)piperazin-1-yl]-1-(4-fluorophenyl)ethanone (26). 26 was prepared in a manner similar to that described for **14** using 1-*tert*-butyl-5-methyl-1*H*-pyrazole-3-carbonyl chloride (49 mg, 0.24 mmol) and 1-(4-fluorophenyl)-2-(piperazin-1-yl)ethanone dihydrochloride (78 mg, 0.26 mmol) and was obtained as a solid (49 mg, 52%). ^{1}H NMR (acetonitrile-d_3, 400 MHz) δ 1.62 (s, 9H), 2.46 (s, 3H), 3.44 (m, 4H), 3.90−4.08 (m, 4H), 4.72 (s, 2H), 6.45 (s, 1H), 7.30 (t, J = 8.8 Hz, 2H), 8.01 (d, J = 8.8 Hz, 2H). LCMS m/z = 387.3 $[M + H]^+$.

2-[4-(4-Chloro-1-methyl-1*H*-pyrazole-3-carbonyl)piperazin-1-yl]-1-(4-fluorophenyl)ethanone (27). 27 was prepared in a manner similar to that described for **14** using 1-(4-fluorophenyl)-2-(piperazin-1-yl)ethanone dihydrochloride (0.37 g, 1.2 mmol) and 4-chloro-1-methyl-1*H*-pyrazole-3-carboxylic acid (0.200 g, 1.20 mmol) to afford the TFA salt of **27** (0.22 g, 50%) as a white solid. Preparation of the HCl salt was as follows. **27** (8.5 g, 23.4 mmol) was dissolved in isopropanol (60 mL), and hydrochloric acid (12 M, 7.41 mL, 89 mmol) was added. The resulting solution was stirred at room temperature overnight. The solid was filtered off and dried to afford **27** HCl salt (8.5 g), mp 204 °C. ^{1}H NMR (DMSO-d_6, 400 MHz) δ 3.05−3.60 (m, 4H), 3.86 (s, 3H), 3.80−4.10 (m, 4H), 4.96−5.12 (m, 2H), 7.48 (t, J = 8.8 Hz, 2H), 8.04−8.13 (m, 3H). LCMS m/z = 365.4/367.4 $[M + H]^+$.

2-[4-(4-Chloro-1-ethyl-1*H*-pyrazole-3-carbonyl)piperazin-1-yl]-1-(4-fluorophenyl)ethanone (28). Compound **28** was prepared in a manner similar to that described for **14** using 4-chloro-1-ethyl-1*H*-pyrazole-3-carboxylic acid (77 mg, 0.44 mmol) and 1-(4-fluorophenyl)-2-(piperazin-1-yl)ethanone dihydrochloride (57 mg, 0.44 mmol) and was obtained as a white solid (114 mg, 68%). ^{1}H NMR (acetonitrile-d_3, 400 MHz) δ 1.42 (t, J = 7.3 Hz, 3H), 3.31−3.50 (m, 4H), 3.90−4.11 (m, 4H), 4.15 (q, J = 7.3 Hz, 2H), 4.72 (s, 2H), 7.28−7.33 (m, 2H), 7.70 (s, 1H), 8.00−8.04 (m, 2H). LCMS m/z = 379.3/381.4 $[M + H]^+$.

2-[4-(4-Chloro-1*H*-pyrazole-3-carbonyl)piperazin-1-yl]-1-(4-fluorophenyl)ethanone (29). 29 was prepared in a manner similar to that described for **14** using 4-chloro-1*H*-pyrazole-3-carboxylic acid (29 mg, 0.2 mmol) and 1-(4-fluorophenyl)-2-(piperazin-1-yl)ethanone dihydrochloride (65 mg, 0.22 mmol) and was obtained as a white solid (37 mg, 53%). ^{1}H NMR (DMSO-d_6, 400 MHz) δ 3.10−4.07 (m, 8H), 5.00 (bs, 2H), 7.45−7.49 (m, 2H), 8.05−8.10 (m, 3H), 13.6 (s, 1H). LCMS m/z = 351.3/353.3 $[M + H]^+$.

1-(4-Fluorophenyl)-2-[4-(1-methyl-5-trifluoromethyl-1*H*-pyrazole-3-carbonyl)piperazin-1-yl]ethanone (30). 30 was prepared in a manner similar to that described for **14** using 1-methyl-5-(trifluoromethyl)-1*H*-pyrazole-3-carboxylic acid (65 mg, 0.33 mmol) and 1-(4-fluorophenyl)-2-(piperazin-1-yl)ethanone dihydrochloride (107 mg, 0.36 mmol) and was obtained as a white solid (143 mg, 100%). ^{1}H NMR (methanol-d_4, 400 MHz) δ 3.48−3.62 (m, 4H), 3.92−4.29 (m, 2H), 4.07 (s, 3H), 4.34−4.69 (m, 2H), 5.03 (s, 2H), 7.19 (s, 1H), 7.34 (t, J = 8.8 Hz, 2H), 8.12 (dd, J = 5.3, 8.8 Hz, 2H). LCMS m/z = 399.2 $[M + H]^+$.

1-(4-Fluorophenyl)-2-[4-(4-iodo-1-methyl-1*H*-pyrazole-3-carbonyl)piperazin-1-yl]ethanone (31). 31 was prepared in a manner similar to that described for **14** using 4-iodo-1-methyl-1*H*-pyrazole-3-carboxylic acid (265 mg, 1.00 mmol) and 1-(4-fluorophenyl)-2-(piperazin-1-yl)ethanone dihydrochloride (295 mg, 1.00 mmol) and was obtained as a white solid (390 mg, 85%). ^{1}H NMR (acetonitrile-d_3, 400 MHz) δ 3.18−3.72 (m, 4H), 3.88 (s, 3H), 4.07−4.52 (m, 4H), 4.79 (s, 2H), 7.33 (t, J = 8.8 Hz, 2H), 7.69 (s, 1H), 8.02 (dd, J = 5.3, 8.8 Hz, 2H). LCMS m/z = 457.3 $[M + H]^+$.

1-(4-Fluorophenyl)-2-[4-(5-methyl-2-phenyl-2*H*-pyrazole-3-carbonyl)piperazin-1-yl]ethanone (32). Compound **32** was prepared in a manner similar to that described for **14** using 3-methyl-1-phenyl-1*H*-pyrazole-5-carboxylic acid (30 mg, 0.15 mmol) and 1-(4-fluorophenyl)-2-(piperazin-1-yl)ethanone dihydrochloride (49 mg, 0.165 mmol) and was obtained as a white solid (32 mg, 52%). ^{1}H NMR (400 MHz, $CDCl_3$) δ 2.35 (s, 3H), 2.60−2.67 (m, 2H), 2.69 (bs, 2H), 3.81 (s, 2H), 3.89 (bs, 2H), 4.16 (bs, 2H), 6.62 (s, 1H), 7.13 (t, J = 8.5 Hz, 2H), 7.38−7.54 (m, 5H), 7.99−8.09 (m, 2H). LCMS m/z = 407.5 $[M + H]^+$.

Biological Assays. [^{125}I]DOI Binding to Recombinant Human 5-HT$_{2A}$ and 5-HT$_{2C}$ Receptors. Radioligand binding assays for human 5-HT$_{2A}$ and 5-HT$_{2C}$ receptors were developed using crude plasma membranes prepared from HEK293 cells stably expressing these receptors. The 5-HT$_2$ agonist [^{125}I]DOI (0.5 nM) was used as radioligand, and nonspecific radioligand binding was determined in the presence of 10 μM cold DOI. Competition experiments were as follows: 95 μL of assay buffer (20 mM HEPES, pH 7.4, 10 mM $MgCl_2$), 50 μL of membranes (5−25 μg of protein), 50 μL of [^{125}I]DOI (0.5 nM final assay

concentration), and 5 μL of test compound serially diluted in DMSO (final concentrations ranging from 1 pM to 10 μM) were added to 96-well plates. Each radioligand competition study consisted of testing 10 different concentrations in which triplicate determinations were performed for each test compound concentration. Plates were incubated for 1 h at room temperature. The assay was terminated by rapid filtration through Perkin-Elmer GF/C filter plates under vacuum pressure using a Brandell cell harvestor, followed by washing filter plates six times with ice-cold wash buffer (50 mM Tris-HCl, pH 7.4). Filter plates were dried at 45 °C in an oven for a minimum of 2 h, 25 μL of BetaScint scintillation cocktail was added to each well, and plates were counted in a Packard TopCount scintillation counter.

Rat Pharmacokinetics. Male Sprague−Dawley rats were dosed orally or intravenously at 10 and 2 mg/kg, respectively, in 80% PEG400 and 20% phosphate buffeted saline. Animals were fasted overnight prior to oral dose administration. Whole blood samples were collected from the jugular vein over a 24 h period postdose. Plasma was prepared from sodium heparin treated whole blood and separated by centrifugation. Plasma samples were assayed using a selective HPLC/MS/MS method. The HPLC/MS/MS was operated in multiple reaction monitoring (MRM) mode under optimized conditions for detection of selected compounds and the internal standard using positive ions formed by electrospray ionization. Quantitation was determined using a weighted regression analysis of peak area ratios of analyte and internal standard. This method provided a lower limit of quantitation of 1 ng/mL and an upper limit of quantitation of 2000 ng/mL. Serial sampling [at 0.25, 0.5, 1, 2, 4, 6, 8, 10, 12, 15, 18, and 21 h after dosing] was used to define the plasma concentration vs time profile.

In Vivo DOI Screen. Male Sprague−Dawley rats weighing between 200 and 350 g were used for all tests. Rats were housed three to four per cage. (*R*)-DOI HCl ($C_{11}H_{16}INO_2 \cdot HCl$) was obtained from Sigma-Aldrich and was dissolved in 0.9% saline. Compounds were dissolved in 100% PEG400. DOI was injected subcutaneously in a volume of 1 mL/kg, while compounds were administered orally in a volume of 1 mL/kg. The "motor monitor" (Hamilton-Kinder, Poway, CA) was used for all activity measurement. This apparatus recorded rears using infrared photobeams. Locomotor activity testing was conducted during the light cycle between 9:00 a.m. and 4:00 p.m. Animals were allowed 30 min of acclimation to the testing room before testing began. In the determination of the effects of compounds on DOI-induced hypolocomotion, animals were first injected with vehicle or the compound (1−10 mg/kg) in their home cages. Twenty-five minutes later, saline or DOI (1 mg/kg) was injected. Ten minutes after DOI administration, animals were placed into the activity apparatus and rearing activity was measured for 10 min.

Rat Sleep Study. All rats (300 ± 25 g; Charles River, Wilmington, MA) were prepared with chronic recording implants for continuous electroencephalograph (EEG) and electromyograph (EMG) recordings and allowed 1 week of recovery prior to treatment. The compounds were compared to vehicle treatment (sterile water) and administered in a repeated measures design, wherein each rat received each treatment in random order via oral gavage. Rats were dosed during the middle of the normal inactive period (3.5 h following lights on). For sleep recordings, animals were connected via a cable and a counterbalanced commutator to a Neurodata model 15 data collection system (Grass-Telefactor, West Warwick, RI). The animals were allowed an acclimation period of at least 48 h before the start of the experiment and were connected to the recording apparatus continuously throughout the experimental period. The amplified EEG and EMG signals were digitized and stored on a computer using SleepSign software (Kissei Comtec, Irvine, CA). EEG and EMG data were scored visually in 10 s epochs for waking (W), REMS, and NREMS. Scored data were analyzed and expressed as time spent in each state per half hour. Sleep bout length and number of bouts for each state were calculated in hourly bins. A "bout" consisted of a minimum of two consecutive epochs of a given state. EEG δ power (0.5−3.5 Hz) within NREMS was also analyzed in hourly bins. The EEG spectra during NREMS were obtained offline with a fast Fourier transform algorithm on all epochs without artifact. Data were analyzed using repeated measures ANOVA. When statistical significance was found from our ANOVAs, *t*-tests were performed comparing all treatment doses to vehicle.

Supporting Information Available: Invitro profiling data of **14** and **27** against a panel of receptors, ion channels, and transporters; differential scanning calorimetry (DSC) graph of **14** and **27**; powder X-ray diffraction (PXRD) of **27**. This material is available free of charge via the Internet at http://pubs.acs.org.

References

(1) Abrams, J. K.; Johnson, P. L.; Hay-Schmidt, A. Serotonergic systems associated with arousal and vigilance behaviors following administration of anxiogenic drugs. *Neuroscience* **2005**, *133*, 983–997.

(2) Hoyer, D.; Clarke, D. E.; Fozard, J. R.; Hartig, P. R.; Martin, G. R.; Mylecharane, E. J.; Saxena, P. R.; Humphery, P. P. International Union of Pharmacology classification of receptors for 5-hydroxytryptamine (serotonin). *Pharmacol. Rev.* **1994**, *46*, 157–203.

(3) Leysen, J. E. 5-HT_2 receptor. *Curr. Drug Targets: CNS Neurol. Disord.* **2004**, *3*, 11–26.

(4) (a) Borbély, A. A.; Trachsel, L.; Tobler, I. Effect of ritanserin on sleep stages and sleep EEG in the rat. *Eur. J. Pharmacol.* **1988**, *156*, 275–278. (b) Monti, J. M.; Jantos, H. Effects of the serotonin 5-$HT_{2A/2C}$ receptor agonist DOI and of the selective 5-HT_{2A} or 5-HT_{2C} antagonists EMD 281014 and SB-243213, respectively, on sleep and waking in the rat. *Eur. J. Pharmacol.* **2006**, *553*, 163–170.

(5) Teegarden, B. R.; Al-Shamma, H.; Xiong, Y. 5-HT_{2A} inverse-agonists for the treatment of insomnia. *Curr. Top. Med. Chem.* **2008**, *8*, 969–976.

(6) Teegarden, B. R.; Li, H.; Jayakumar, H.; Strah-Pleynet, S.; Dosa, P. I.; Selaya, S. D.; Kato, N.; Elwell, K. H.; Davidson, J.; Cheng, K.; Saldana, H.; Frazer, J. M.; Whelan, K.; Foster, J.; Espitia, S.; Webb, R. R.; Beeley, N. R. A.; Thomsen, W.; Morairty, S. R.; Kilduff, T. S.; Al-Shamma, H. A. Discovery of 1-[3-(4-bromo-2-methyl-2*H*-pyrazol-3-yl)-4-methoxy-phenyl]-3-(2,4-difluoro-phenyl)-urea (nelotanserin) and related 5-hydroxytryptamine$_{2A}$ inverse agonists for the treatment of insomnia. *J. Med. Chem.* **2010**, *53*, 1923–1936.

(7) Al-Shamma, H. A.; Anderson, C.; Chuang, E.; Luthringer, R.; Grottick, A. J.; Hauser, E.; Morgan, M.; Shanahan, W.; Teegarden, B. R.; Thomsen, W. J.; Behan, D. Nelotanserin, a novel selective human 5-hydroxytryptamine$_{2A}$ inverse agonists for the treatment of insomnia. *J. Pharmacol. Exp. Ther.* **2010**, *332*, 281–290.

(8) Rosenberg, R.; Seiden, D. J.; Hull, S. G.; Erman, M.; Schwartz, H.; Anderson, C.; Prosser, W.; Shanahan, W.; Sanchez, M.; Chuang, E.; Roth, T. APD125, a selective serotonin 5-HT_{2A} receptor inverse-agonist, significantly improves sleep maintenance in primary insomnia. *Sleep* **2008**, *31*, 1663–1671.

(9) Fletcher, S. R.; Burkamp, F.; Blurton, P.; Cheng, S. K. F.; Clarkson, R.; O'Connor, D.; Spinks, D.; Tudge, M.; van Niel, M. B.; Patel, S.; Chapman, K.; Marwood, R.; Shepheard, S.; Bentley, G.; Cook, G. P.; Bristow, L. J.; Castro, J. L.; Hutson, P. H.; Macleod, A. M. 4-(Phenylsulfonyl)piperidines: novel, selective, and bioavaliable 5-HT_{2A} receptor antagonists. *J. Med. Chem.* **2002**, *45*, 492–503.

(10) (a) Ladduwahetty, T.; Boase, A. L.; Mitchinson, A.; Quin, C.; Patel, S.; Chapman, K.; Macleod, A. M. A new class of selective, non-basic 5-HT_{2A} receptor antagonists. *Bioorg. Med. Chem. Lett.* **2006**, *16*, 3201–3204. (b) Bartoszyk, G. D.; van Amsterdam, C.; Böttcher, H.; Seyfried, C. A. EMD 281014, a new selective serotonin 5-HT_{2A} receptor antagonist. *Eur. J. Pharmacol.* **2003**, *473* (2−3), 229–230.(c) van Amsterdam, C.; Sedman, E.; Bartoszyk, G.; Hellmann, J.; von Landengerb, F.. Use of N-(Indolcarbonyl-)piperazine Derivatives. WO2003045392, June 5, 2003.

(11) Adams, J. W.; Ramirez, J.; Shi, Y.; Thomsen, W.; Frazer, J.; Morgan, M.; Edwards, J. E.; Chen, W.; Teegarden, B. R.; Xiong, Y.; Al-Shamma, H.; Behan, D. P.; Connolly, D. T. APD791, a novel 5-hydroxytryptamine 2A receptor antagonist: pharmacological profile, pharmacokinetics, platelet and vascular biology. *J. Pharmacol. Exp. Ther.* **2009**, *331*, 96–103.

(12) Xiong, Y.; Teegarden, B. R.; Choi, J. K.; Strah-Pleynet, S.; Decaire, M.; Jakakumar, H.; Dosa, P. I.; Casper, M.; Pham, L.; Feichtinger, K.; Ullman, B.; Adams, J.; Yuskin, D.; Frazer, J.; Morgan, M.; Sadeque, A.; Chen, W.; Webb, R. R.; Connolly, D. T.; Semple, G.; Al-Shamma, H. Discovery and structure−activity relationship of 3-methoxy-*N*-(3-(1-methyl-1*H*-pyrazol-5-yl)-4-(2-morpholinoethoxy)phenyl)-benzamide (APD791): a highly selective 5-hydroxytryptamine$_{2A}$ receptor inverse agonist for the treatment of arterial thrombosis. *J. Med. Chem.* **2010**, *53*, 4412–4421.

(13) Xiong, Y.; Cherrier, M.; Choi, J. K.; Dosa, P. I.; Smith, B. M.; Strah-Pleynet, S.; Ullman, B.; Teegarden, B. Pyrazole Derivatives as Modulators of the 5-HT$_{2A}$ Serotonin Receptor Useful for the Treatment of Disorders Related Thereto. PCT/US2007/021182, WO2008042388, April 10, 2008.

(14) Cheng, Y. C.; Preusoff, W. H. Relationship between the inhibition constant (K_i) and the concentration which causes 50% inhibition (IC_{50}) of an enzymatic reaction. *Biochem. Pharmacol.* **1973**, *23*, 3099–3108.